77 GHz Radar Transceiver with Dual Integrated Antenna Elements

Jürgen Hasch, Uwe Wostradowski, Stefan Gaier, Thomas Hansen
Robert Bosch GmbH, CR/ARE1, Corporate Sector Research and Advance Engineering
P.O. Box 10 60 50, D-70049 Stuttgart, Germany
Email: juergen.hasch@de.bosch.com

***Abstract*—A complete radar transceiver for 77 GHz with two integrated antenna elements is presented. Based on a previously published design [1], two of the transmit and receive channels of the transceiver are supplemented with integrated antenna elements. The antennas exhibit a well defined antenna pattern with an efficiency of better than 50%.**

I. Motivation

Modern driver assistance systems for ACC (Adaptive Cruise Control) or PSS (Predictive Safety Systems) functions are often based on radar sensors [2]. Recent implementations are using millimeter-waves in the 76.5 GHz band for long range applications or the newly available 77-79 GHz band for medium and short range applications, respectively [3]. Due to the availability of modern SiGe technologies with f_T and f_{max} of more than 200 GHz, the realization of the millimeter-wave part of the radar sensor has become feasible as a highly-integrated circuit, superseding the costly and difficult traditional discrete component assembly of such systems.

One still remaining bottleneck is a millimeter-wave capable packaging of the integrated circuit, in order to transfer high-frequency signals from the chip to the antenna system and back. In order to avoid expensive packages, wire bonding is often used, but this typically leads to high insertion losses for the 77 GHz signals.

One way to avoid elaborate packaging would be to integrate the antenna itself on the chip. However, for automotive radar systems, a well defined antenna pattern accompanied by a good antenna efficiency is required. Simply placing an antenna element on the chip typically leads to marginal results. Most of the millimeter-wave energy is either dissipated in the low-resistivity bulk silicon or – for patch-type antenna configurations that shield the bulk substrate – in the backend interconnect layers, due to the very thin substrate layer.

Investigations into integrated antenna elements have been made by a number of authors. A number of approaches have been examined, for example adding an additional thick dielectric layer on top of the chip [4] or backside micromachining [5] the silicon chip. However, these additional technology steps require processing of a complete wafer and are often not applicable for mass production.

In the approach presented here, no further processing steps are necessary for the silicon wafer. All additional steps are based on available standard packaging technology, allowing an easy exploitation of the antenna concept.

II. Integrated Radar Transceiver

In order to investigate the proposed antenna concept and to verify it's performance in a real world radar system, the antennas were integrated together with an existing transceiver circuit in a 200 GHz f_T SiGe technology [6].

The four channel radar transceiver circuit itself has been described previously in [1]. It includes a VCO, a power amplifier, two frequency divider chains and four receive mixers in order to provide two transmit and four receive channels. The VCO can be frequency modulated for FMCW operation, together with the frequency-divider chain an external phase-locked-loop can be realized.

In this version of the transceiver, two of the channels are configured to realize a monostatic radar system, using on-chip rat-race couplers for transmit/receive separation. The two antenna elements are connected to the monostatic transmit/receive channels, while the two remaining receive-only channels are not used in this configuration. The block diagram of the transceiver is shown in figure 1.

The two antennas are spaced $\lambda/2$ free space distance apart to allow direction of arrival (DOA) estimation of a target detected by the radar.

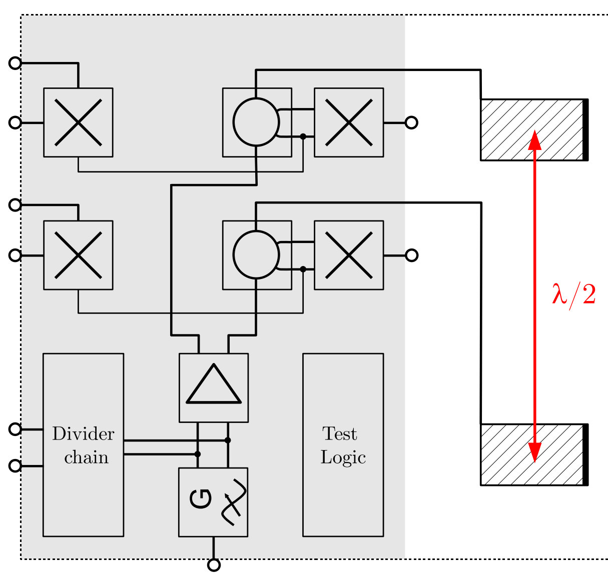

Fig. 1. Overall block diagram of the transceiver circuit with the two antenna elements attached

III. Antenna Concept

The on-chip antenna elements are based on a shorted quarter-wavelength microstrip line, formed by the top and bottom metal layers of the standard backend technology. The microstrip line thereby acts as a patch antenna with one radiating slot, with its resonating frequency determined by the length l. This is shown in figure 2.

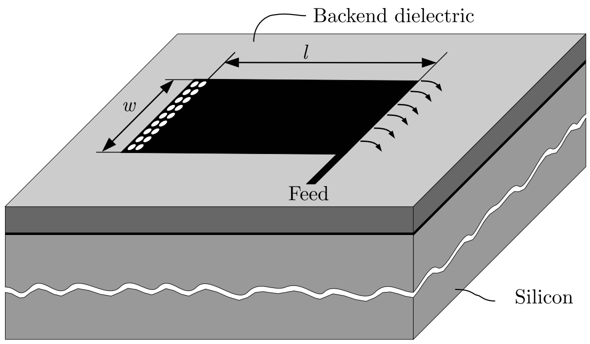

Fig. 2. Shorted quarter-wavelength antenna patch

By feeding the patch at the open end and making the width w much smaller than the resonant length l of the patch, a high input impedance of more than $100\,\Omega$ at resonance frequency can be achieved. Because of the thin substrate thickness between the ground plane and the patch element, typically in the $10\,\mu$m range, the radiation efficiency of the antenna is quite low and most of the energy is dissipated due to conductor and dielectric losses. Typically much less than 10% of the energy applied to the antenna port gets radiated into free space.

The antenna performance can be drastically improved by introducing an additional half-wavelength long parasitic resonator positioned directly above the patch element, as shown in figure 3. In our approach described here, a small quartz glass substrate is placed directly on top of patch antenna element on the chip. On the top side of the quartz glass metallization for the parasitic resonator element is realized using thin film technology.

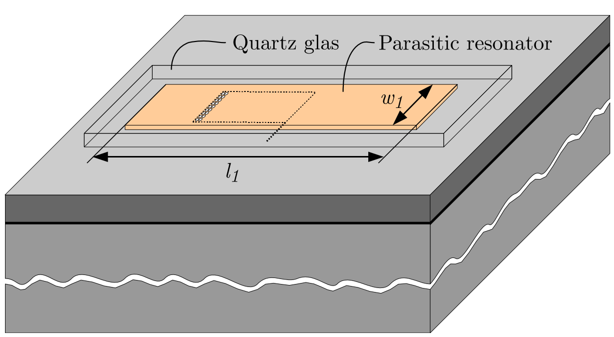

Fig. 3. Parasitic resonator placed above antenna patch

By placing the parasitic resonator in close proximity of the patch, it is electromagnetically coupled to the resonator, achieving directed radiation with high efficiency.

The parasitic resonator also adds another pole to the input reflection coefficient S_{11} of the antenna. By optimizing the dimensions l,w of the integrated quarter-wavelength patch element, the height of the quartz glass and the dimensions l_1,w_1 of the resonator, a broadband input match can be achieved, as shown in figure 4. For an optimum design of the

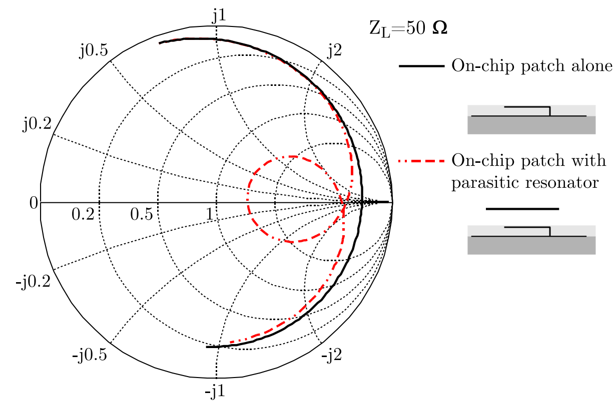

Fig. 4. Simulated input impedance of the antenna element

antenna, the finite size of the quartz glass and the chip have to be taken into account. Careful design allows the effect of these parameters on the antenna performance to be minimized.

In order to enable angular direction of arrival estimation, a monopulse antenna configuration using two antennas was realized. Therefore, the two antennas were spaced at a freespace distance of $\lambda/2$ apart of each other. Using the phase difference between the two receive channels, the direction of arrival of a reflected radar signal can be determined.

IV. On-Chip Measurement Concept

A major challenge for an on-chip antenna system is to measure the antenna input reflection coefficient S_{11} and the RF output power of the transceiver over frequency, directly at the antenna feed. Measurements using an onwafer probing setup can strongly influence the antenna characteristics. This is due to metallic structures like the prober head or the microscope optics, which are positioned in close proximity to the antenna under investigation itself. Also, the output power of the transceiver circuit can only be measured by probing a design having contact pads instead of an antenna structure.

Therefore, an in-situ approach to measure output power and reflection coefficient directly on-chip has been implemented. A directional coupler and two power sensors were designed and placed directly at the antenna feed, in order to measure the power of injected and reflected signals at the antenna port.

In addition, test structures for the directional coupler and the power sensors have been realized on the same chip. RF contact pads allow for onwafer-probing and characterization. This way the on-chip measurement circuit could be calibrated to the actual performance of the directional coupler and power sensors. Especially temperature changes will cause drifts of the power sensors that need to be taken into account.

V. Assembly

The chip including transceiver and antenna elements has been fabricated in Infineon Technologies B7HF process with overall dimensions of 3.25 x 3.25 mm. The fabricated chip was glued on an aluminium heatsink and contacted to a surrounding PCB using gold wirebonds. As no millimeter-wave signals need to be transmitted over the bond wires, relaxed bonding parameters could be employed.

The PCB contains all necessary electronic components to control the radar transceiver chip. In addition to power supply and signal conditioning circuitry, a PLL is used to stabilize the millimeter-wave oscillator and to create a highly linear FMCW modulation for radar operation. The receive channels are connected to AD-converters and a microcontroller is used to control the radar operation and process the receive signals.

Figure 5 shows the assembled chip, wirebonded to the PCB. The two quartz glass resonators for the antenna are already mounted on top of the chip.

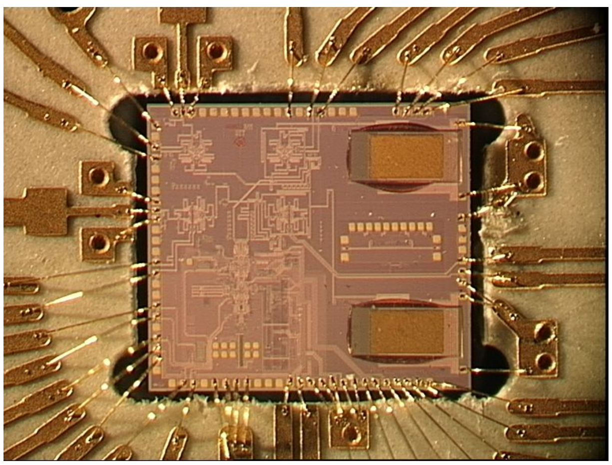

Fig. 5. Complete radar transceiver with dual antenna

Figure 6 shows a closeup view of the resonator. The quartz glass has been placed on top of the chip using a standard micro placer and is fixed with standard epoxy based glue. The size of the quartz glass is slightly larger than the half-wavelength resonator structure it carries. Because quartz glass is transparent, the resonator structure can be easily placed accurately over the on-chip patch element using placer marks.

The directional coupler used for on-chip power measurement is placed directly at the antenna feed, is however concealed in the picture by the epoxy glue used to fixate the quartz glass.

VI. Measurement

To calibrate the on-chip measurement circuit, consisting of an integrated directional coupler with power sensors for the forward and backward traveling waves, an onwafer-probing setup consisting of a power meter, a network analyzer, a sliding short and a adjustable attenuator was used.

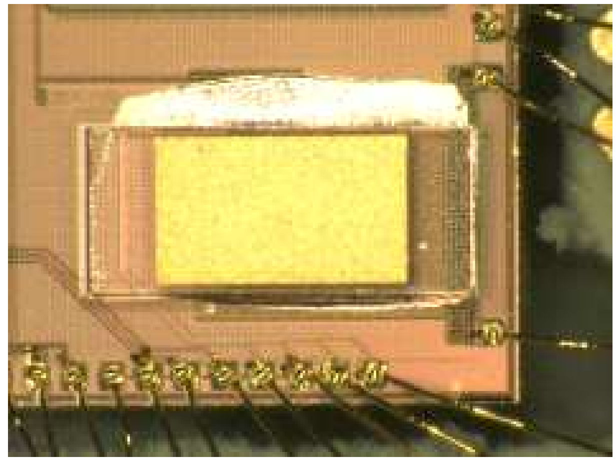

Fig. 6. Close-up view of the resonator element mounted on the transceiver chip

The coupling factor of the directional coupler over frequency was determined using the network analyzer. Using the adjustable attenuator and the power meter, the measurement range of the integrated power sensors was found to be from -7 to +10 dBm over frequency, wit a measurement uncertainty in the reflection measurement of about 3 dB. The transceiver output power was then measured at both antenna feed points. It showed at output power between +7 to +5 dBm and +6 to +5 dBm respectively, measured in the frequency range of 76 to 77 GHz. Due to a longer feed line connecting second antenna, the slightly lower output power can be attributed to the additional feed line attenuation. The input reflection coefficient for the integrated antenna was found to be better than -20 dB.

A single on-chip antenna was measured using a measurement setup on a rotating table in an anechoic chamber. The radar transceiver-chip was operated as transmitter with both antennas operating. A 20 dB standard horn antenna connected to an external W-band mixer and a spectrum analyzer was used as receiver. The antenna pattern in the H-plane was measured and compared to the results of a 3D fullwave simulation. As shown in figure 7, simulation and measurement achieve a very good match.

An accurate determination of the antenna efficiency is difficult. Simulations using a 3D fullwave solver and measurements comparing on-chip with off-chip antennas indicate an overall antenna efficiency of better than 50%. Further investigations to reduce the uncertainty of the measurements are planned.

Finally, the direction of arrival estimation performance was investigated. Therefore the transceiver was operated in FMCW mode with a corner reflector as radar target. The measurement was performed in an anechoic chamber with a rotating table, so the performance over an angular range could be automatically measured.

The base band signals of both receiver channels were captured and the phase difference between the channels was

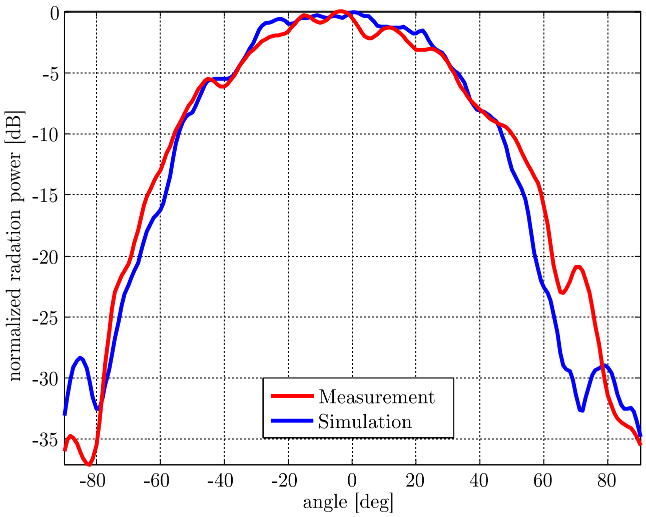

Fig. 7. Normalized antenna pattern of a single antenna element

calculated. Figure 8 shows the plotted phase difference over a range of $\pm 50°$. The curve shows a quite linear behavior, only with some ripples as the angle increases. These ripples are caused by additional reflections of the radar signal at components on the PCB and in the radar housing.

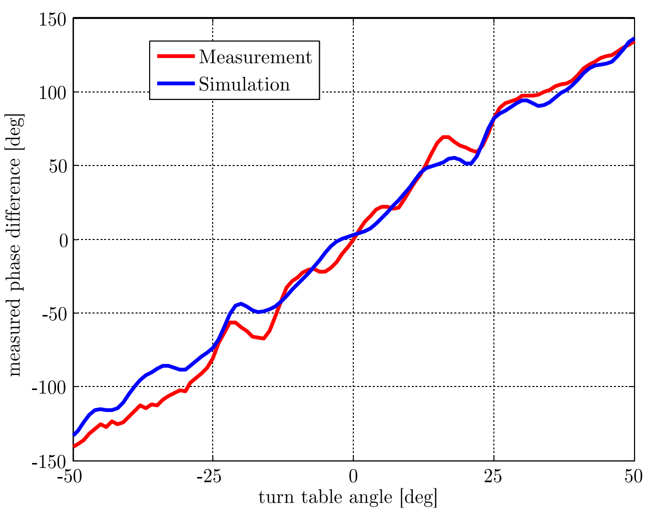

Fig. 8. Measured phase difference between the two channels for a single radar target

VII. Conclusion

A 77 GHz two-channel radar transceiver with integrated antennas was presented. The antennas exhibits well defined characteristics with an efficiency above 50%. By using two $\lambda/2$-spaced antennas, a direction of arrival estimation can be achieved over an angular range of $\pm 50°$.

This approach allows a low-cost realization of a radar system without the need for millimeter-wave packaging or a high-end PCB substrate. No additional process steps for chip manufacturing are necessary and all steps shown require only readily available standard equipment.

Acknowledgment

The authors would like to thank H.-P. Forstner and R. Lachner of Infineon Technologies for design support and fabrication of the chips. This work was in part supported by the German Federal Ministry of Education and Research (BMBF) under contract 13N9820-13N9824 *Radar on Chip for Cars* (RoCC).

References

[1] H. Forstner, H. Knapp, H. Jager, E. Kolmhofer, J. Platz, F. Starzer, M. Treml, A. Schinko, G. Birschkus, J. Bock, K. Aufinger, R. Lachner, T. Meister, H. Schafer, D. Lukashevich, S. Boguth, A. Fischer, F. Reininger, L. Maurer, J. Minichshofer, and D. Steinbuch, “A 77 ghz 4-channel automotive radar transceiver in sige,” in *Radio Frequency Integrated Circuits Symposium, 2008. RFIC 2008. IEEE*, 17 2008-April 17 2008, pp. 233–236.

[2] D. Freundt and B. Lucas, “Long range radar sensor for high-volume driver assistance systems market,” in *SAE World Congress & Exhibition*, 2008.

[3] H.-L. Bloecher, A. Sailer, G. Rollmann, and J. Dickmann, “79 ghz uwb automotive short range radar spectrum allocation and technology trends,” *Advances in Radio Science*, vol. 7, pp. 61–65, 2009. [Online]. Available: http://www.adv-radio-sci.net/7/61/2009/

[4] R. Carrillo-Ramirez and R. Jackson, “A highly integrated millimeter-wave active antenna array using bcb and silicon substrate,” *Microwave Theory and Techniques, IEEE Transactions on*, vol. 52, no. 6, pp. 1648–1653, June 2004.

[5] I. Papapolymerou, R. Franklin Drayton, and L. Katehi, “Micromachined patch antennas,” *Antennas and Propagation, IEEE Transactions on*, vol. 46, no. 2, pp. 275–283, Feb 1998.

[6] J. Bock, H. Schafer, K. Aufinger, R. Stengl, S. Boguth, R. Schreiter, M. Rest, H. Knapp, M. Wurzer, W. Perndl, T. Bottner, and T. Meister, “Sige bipolar technology for automotive radar applications,” in *Bipolar/BiCMOS Circuits and Technology, 2004. Proceedings of the 2004 Meeting*, Sept. 2004, pp. 84–87.